In: Information Processing in the Somatosensory System. Eds: O. Franzen and J. Westman, Wenner-Gren International Symposium Series, MacMillan Press, 1991.

5

Encoding of Shape in the Responses of Cutaneous Mechanoreceptors

Mandayam A. Srinivasan and Robert H. LaMotte

Tactile detection of surface features of objects is essential for successful exploration and manipulation of our environment. Primates predominantly use fingerpads for exploring small features, owing to the high density of cutaneous mechanoreceptors (Johansson and Vallbo, 1979; Darian-Smith and Kenins, 1980) which results in high spatial resolution, as well as due to the dexterity and fine motion control achieved with multiple degrees of freedom to move the fingertip. For humans, the normal contact forces used and the compliance of the fingertip result in contact regions whose overall diameter measures about a centimeter. At any time during contact, the information conveyed by cutaneous mechanoreceptors pertain only to the features within the contact region, thereby limiting the largest lengthscale of the surface features represented in cutaneous information to be of the order of centimeters. The smallest lengthscale is governed by the response thresholds of mechanoreceptors, which can be as low as fractions of a micron (LaMotte and Srinivasan, 1990). In this article we are concerned with millimeter to centimeter sized surface features of rigid objects, the shape of which can be detected from purely cutaneous information.

From an information processing point of view, tactile sensing of shape can be seen as the flow of information from the object surface to the brain. The path of this flow consists of several stages, with a different representation for shape at each stage. Some of the stages relevant to our purpose here are the geometry of the object itself, mechanical loading on the skin surface, stress and strain fields within the skin (especially at the receptor locations), spatio-temporal patterns of action potentials in afferent fibers, and further transformations within the nervous system. At each of these stages, the representation of shape can be achieved by several candidates. The problem of understanding how shape is detected through touch requires an investigation of what representations are actually used by the somatosensory system at each stage of the information flow.

* We gratefully acknowledge the technical assistance of Jim Whitehouse. This research was funded by ONR contract N0014-88-K-0604, NIH grant NS15888, and NIH FIRST Investigator Award NS27420.

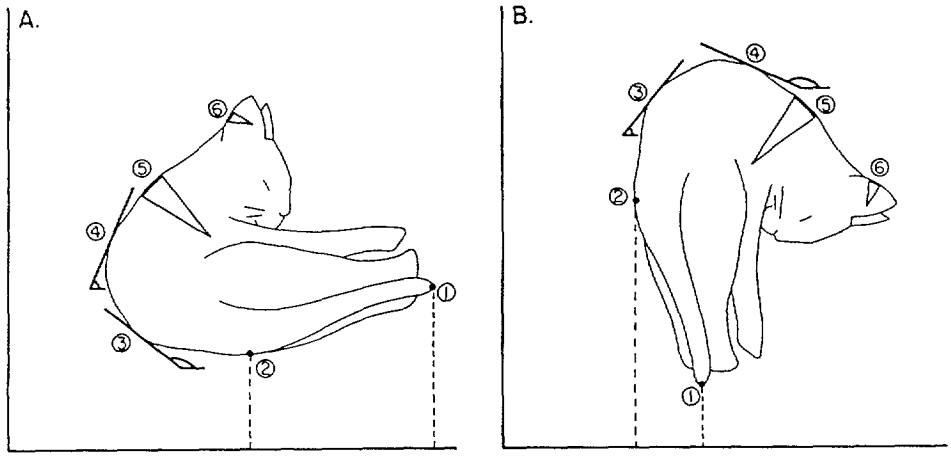

Fig. 1. Representations of object geometry. Three possible representations are shown -- the coordinates of each point on the surface (for example, cartesian coordinates of points 1 and 2), the surface slope (indicated by the angles of inclination of the tangents at points 3 and 4, with respect to the horizontal) as a function of the coordinates, and the local curvature (reciprocal of the radius of the circle fitted to the surface profile at the point of interest, as indicated by the arcs for points 5 and 6) as a function of the distance along the surface. The figure on the right is obtained by a translation and a 90° rotation of the one on the left, and shows that the first two representations are altered, while the third 'intrinsic' representation remains invariant.

Three possible representations of the geometry of the object surface are depicted in Fig. 1A. The first possibility is that each point on the object surface could be identified in terms of its *coordinates* from some fixed axes. An example of such a representation is the determination of surface shape with a profilometer, where a stylus moves over the surface of the object with its tip in continuous contact, and the successive positions of the tip determines the object surface profile. The second possibility is expressing the *local slope* at each point on the object surface as a function of the coordinates of the point. This representation has been found to be relevant in the determination of shape from shading (either by human or robot vision), because the path of the reflected light from a surface depends on the local surface slope, in addition to the direction of incident light (Horn, 1986). The form of these two representations depends on the chosen coordinate system, and hence the representations are not invariant when the object is translated or rotated (Fig. 1). The third representation is obtained by expressing the *local curvature* (reciprocal of the radius of the circle that can be fitted locally to the surface profile of a given cross section) of the surface as a function of the coordinates expressed in terms of distance along the surface. Based on the fundamental results obtained by Gauss (1827), it is known from differential geometry that such a function determines the form of a curve, or more generally a surface, uniquely. This representation is termed 'natural' or 'intrinisic' because it does not make reference to a particular system of coordinates, and therefore has the advantage that it is invariant with respect to translation and rotation of the object. It is this representation that seems to be particularly relevant

to the coding of shape by cutaneous mechanoreceptors, as indicated by the neurophysiological evidence presented below.

1. Responses to step shapes

In our studies on the encoding of smoothly contoured shapes by mechanoreceptive afferents (LaMotte and Srinivasan 1987a,b; Srinivasan and LaMotte 1987), we employed a series of transparent flat plates cast in epoxy, each having an increase in thickness (a step) in the middle so that half of the plate was thicker than the other (Fig. 2A). The cross sectional shape of the step approximated that of a half-cycle of a sinusoid (Fig. 2B). These steps were mounted on a servo-controlled mechanical stimulator which applied the steps to the fingerpad of the anesthetized monkey. Evoked action potentials were recorded from slowly adapting (SA) and Meissner corpuscle rapidly adapting (RA) afferent fibers innervating the fingerpad. One set of experiments consisted of indentations by each step at a succession of lateral positions in increments of 0.1 to 0.5 mm across the fiber's receptive field. Each indentation consisted of a vertical indentation ramp of 4mm/sec that was continued till a force of 20 g wt was reached, after which the force was maintained constant for 2 to 6 sec., followed by withdrawal of the step. The response was plotted as a function of the relative positions of the most sensitive spot (MSS) of the receptive field on the step to obtain a 'spatial response profile' (Figs. 2C and D).

The major features of the SA response profiles to a single step can be readily related to the geometry of the region of the step that is indenting the MSS of the SA's receptive field (top of Fig. 2C): (a) the base response to the flat part of the step on either side of the sinusoidal portion; (b) peak response when the sharpest part of the step is on the MSS; (c) a very low response when the MSS is under the concave portion of the step, especially for the steep steps under which a gap is formed between the skin surface and the step. These results show a direct relationship between the responses of the SA and the changes in the curvature (measured relative to the resting state) of the skin surface at the MSS – both are maximum under the sharpest part of the step, medium under the flat part, and minimum at the gap. The exquisite sensitivity of the SA to the change in skin surface curvature is further illustrated by comparing the response profiles to different steps. While the base response is almost the same for all the steps (except for some intertrial adaptation effects), the gross difference in the maximum curvature between steps 3 and 4 results in a large difference in the peak responses, and even the fine differences between maximum curvatures of step pairs 2,3 and 4,5 are reflected in the corresponding peak responses.

In contrast, the analogous results for even the RA that discriminated the steps best (Fig. 2D – the other RAs had almost flat response profiles to all the steps), shows that it is much poorer than a typical SA in discriminating shapes under stationary indentations. The RA spatial response profiles seem to reflect the skin deflection profiles, correlating with the lack of significant differences in the deflection profiles for the steps within the groups of (0–3) and (4–5), which were observed using a microscope and a videocamera. The data on the responses of RAs to indentations with probes (Knibestöl, 1973,

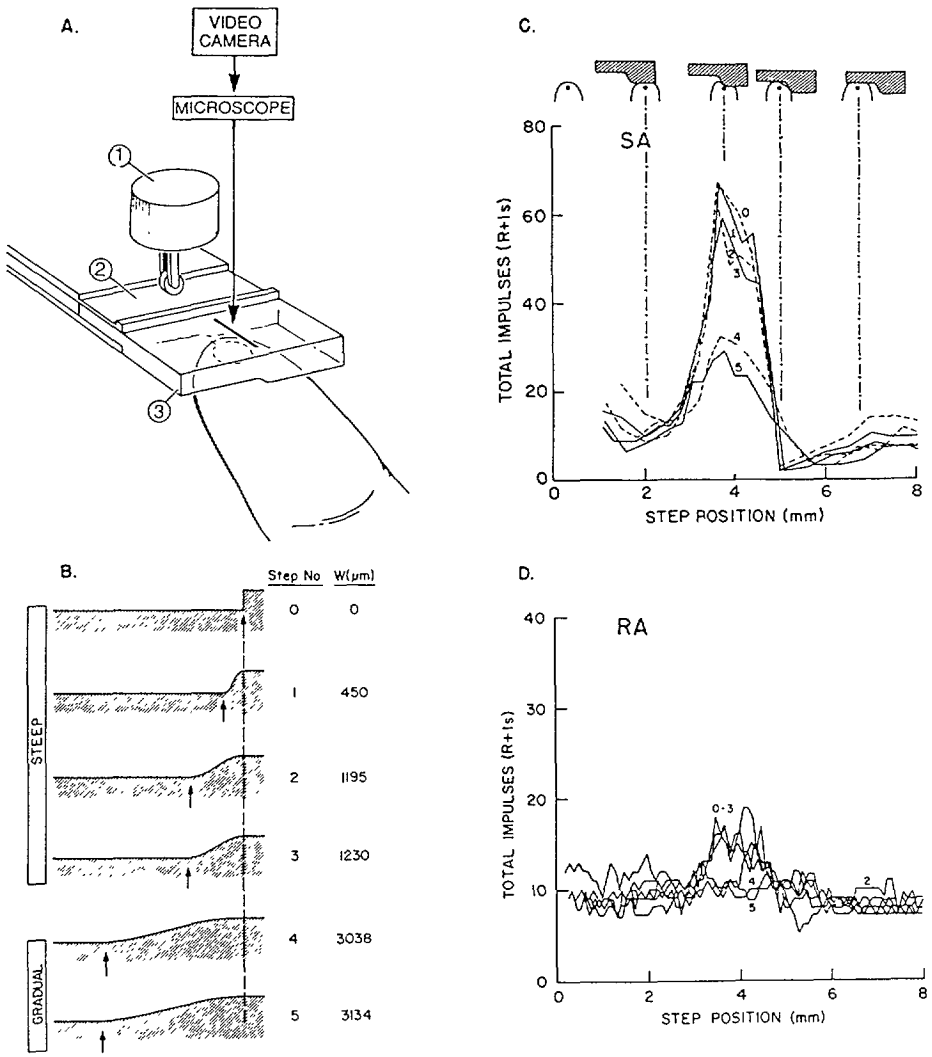

Fig. 2. Peripheral neural responses of mechanoreceptive afferents to indentation by sinusoidal steps. **A.** Experimental setup. Passive monkey fingerpad is indented by each transparent step (3) mounted onto a servocontrolled stimulator through a lever (2) that is in contact with a force transducer (1). A videocamera mounted on a dissection microscope was used in correlating the step position on the skin with the neural response. **B.** Cross-sectional profiles of the step shapes (numbered 0-5). While the height of each step was fixed at 0.5mm, the width (i.e. half-cycle wavelength W, defined as the horizontal distance between the arrow and the dashed vertical line) was varied. **C.** Spatial response profiles of a typical SA to each of the steps. The cumulative number of impulses at 1 sec. after the end of the ramp is plotted as a function of the position of the steps on the skin. The schematic above (not to scale) indicates some of these positions relative to the location of the most sensitive spot (MSS) on the receptive field. **D.** Spatial response profiles of the RA that discriminated the steps best. Figures B,C, and D are plotted to the same horizontal scale. Adapted from LaMotte and Srinivasan (1987a), and Srinivasan and LaMotte (1987).

Pubols and Pubols, 1976) show that the discharge rate (impulses per sec.) is a sigmoidal function of the velocity of indentation, and that a linear relation between the discharge rate and the vertical velocity of MSS is a valid first approximation. It can then be shown that the spatial response profile must match the skin deflection profile (LaMotte and Srinivasan, 1987b). Thus, the RA may be seen as conveying information about the shape of the skin profile under the object, which is the same as the shape of the object surface only in the regions of contact. The increased responses to the sharpest part of the steps (0–3) indicates that the RA might possess a sensitivity to the rate of curvature change at the MSS (as indicated by the responses to stroking of steps described below) which, for stationary indentations, is nonzero only in the very beginning of the ramp phase.

We have also obtained the responses of SAs and RAs to the sinusoidal steps stroked at various velocities across the fingerpad under constant compressive force (LaMotte and Srinivasan, 1987a,b). The results show that for both SAs and RAs, the peak discharge rate under the sharp portion of the steps depends directly on the curvature and stroke velocity of the steps. In fact, the RA discharge rates could discriminate better than the SAs, the differences in curvature between the steps stroked at the same velocity, demonstrating their sensitivity to the rate of change of curvature. These results together with the earlier observations from probe indentation experiments (e.g., Knibestöl, 1973,1975; Pubols and Pubols, 1976) gave rise to the following hypotheses (Srinivasan and LaMotte, 1987):

1. **SA.** The discharge rate of an SA is a function of the displacement and velocity perpendicular to the skin surface, as well as the amount and rate of change in curvature of the skin at the MSS in its receptive field. The higher the value of any of these four quantities, the higher the discharge rate; however, when the rate of change of curvature is negative, the SA becomes silent.
2. **RA.** The discharge rate of an RA is a function of the velocity perpendicular to the skin surface, and the rate of curvature change at the MSS in its receptive field. The higher the magnitude of either of these, the higher the discharge rate.

These hypotheses can be shown to explain the SA and RA responses to a wide range of stimuli such as indentation by probes, indentation and stroking by sinusoidal steps, and indentation by gratings consisting of rectangular bars and gaps used by Phillips and Johnson (1981a). For example, the higher response of the SA to the edge of a bar than to the flat part, is due to the higher change in skin surface curvature under the edge as the skin conforms to it; the higher the gap width, the better the conformation, resulting in a higher response to the edge. The similarity in the spatial response profiles of the RAs to the corresponding skin deflection profiles under the gratings is a consequence of the discharge rate of the RAs being approximately proportional to the normal velocity of the MSS, as explained above.

2. Responses to cylindrical bars

In order to test the above hypotheses in a simple and direct manner, we chose to use cylindrical bars of differing radii of curvature, and a flat plate as stimuli. Responses from SAs and RAs were recorded to vertical indentations of the MSS by the curved surface of each cylinder using an electromechanical stimulator, under force control (150 g wt/sec ramp, 20g wt steady force for 2 sec.). The SA response rasters showing the occurrence of action potentials

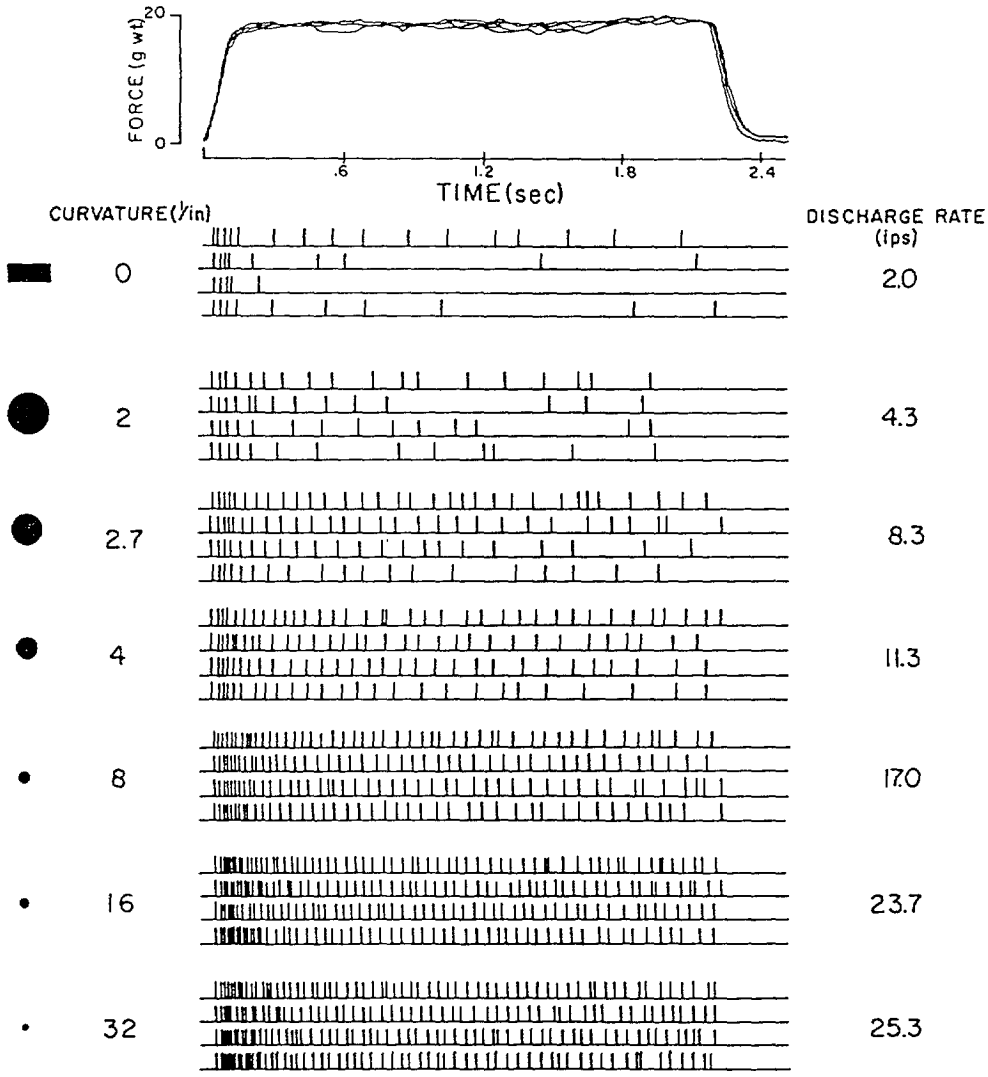

Fig. 3. SA responses to indentations of the MSS by a flat surface and cylinders of differing radii. The variation of contact force over time during four separate indentations is shown on top. The responses of the SA to the indentations of each cylinder are shown below, with each vertical tick representing an action potential recorded at the corresponding time. The curvature of the cylinders (reciprocal of the radius in inches) is shown on the left and the corresponding average discharge rate (impulses per sec.) during the constant force phase is shown on the right.

over time during four repeated indentations by each of the cylinders is shown in Fig. 3. For all the recorded SAs, the discharge rate increased with increases in the curvature of the indenting cylinder, both during the ramp and steady phases. Also, none of the RAs whose responses were recorded were as sensitive to the variations in the curvatures. The limited discriminability of the RA may be due to its response to curvature rate at the MSS, which is nonzero only in the beginning of the ramp phase when the skin surface bends to conform to the curved surface of the cylindrical bar. In one experiment, we obtained tuning thresholds (expressed as amplitude in microns needed to elicit 1 impulse/stimulus cycle) of an RA to 30 Hz sinusoidal vibrations by the cylindrical bars. It was found that the higher the curvature, the lower were the thresholds. These results strongly support the proposed hypotheses on the SA and RA responses.

3. Responses to corrugated surfaces

Commonly encountered surface shapes generally consist of both convexities and concavities. To investigate the peripheral neural representation of such surface shapes, a smooth curvature pattern of alternating convex and concave cylindrical surfaces of differing curvature was designed such that the surface slope was continuous (Fig. 4). A computer controlled numerical milling machine was used to obtain the desired surface shape to tolerances of 0.001 in. on an aluminum specimen. No surface texture could be felt on the milled surface. Accurate transparent epoxy copy of the surface was mounted on the servo-controlled mechanical stimulator, and was stroked across the fingerpads of anesthetized monkeys under force control (20 g wt.) at a constant velocity of 10 mm/sec. Spatial response rasters of typical SA and RA afferents innervating the fingerpad are shown in Fig. 4. Both responded with bursts and pauses, responding only when the convex portions of the corrugations were on the MSS. The width and the average frequency of the responses of both SAs and RAs directly related to the wavelength and radius, respectively, of the corrugation that was on the MSS. The RA responded only to the leading half of the convex portion, i.e., when the MSS was being indented. The SA responded to both halves of the corrugation, with significantly higher frequency to the leading half. These results are entirely consistent with the hypotheses proposed earlier.

4. Mechanism for curvature coding

Because of the compliance of the skin and its substrata, the skin surface conforms to the surface of the object in the regions of contact, and reflects the shape of the object in those regions. We have shown that the amount and the rate of change of the skin surface curvature are represented in the discharge rates of SAs and RAs. The question then is, what is the mechanism by which such a transformation of representation might take place. The answer requires an understanding of the mechanical loading imposed by the object on the skin surface, transmission of the mechanical signals through the skin to the mechanoreceptors, and the transduction of the relevant stresses and/or

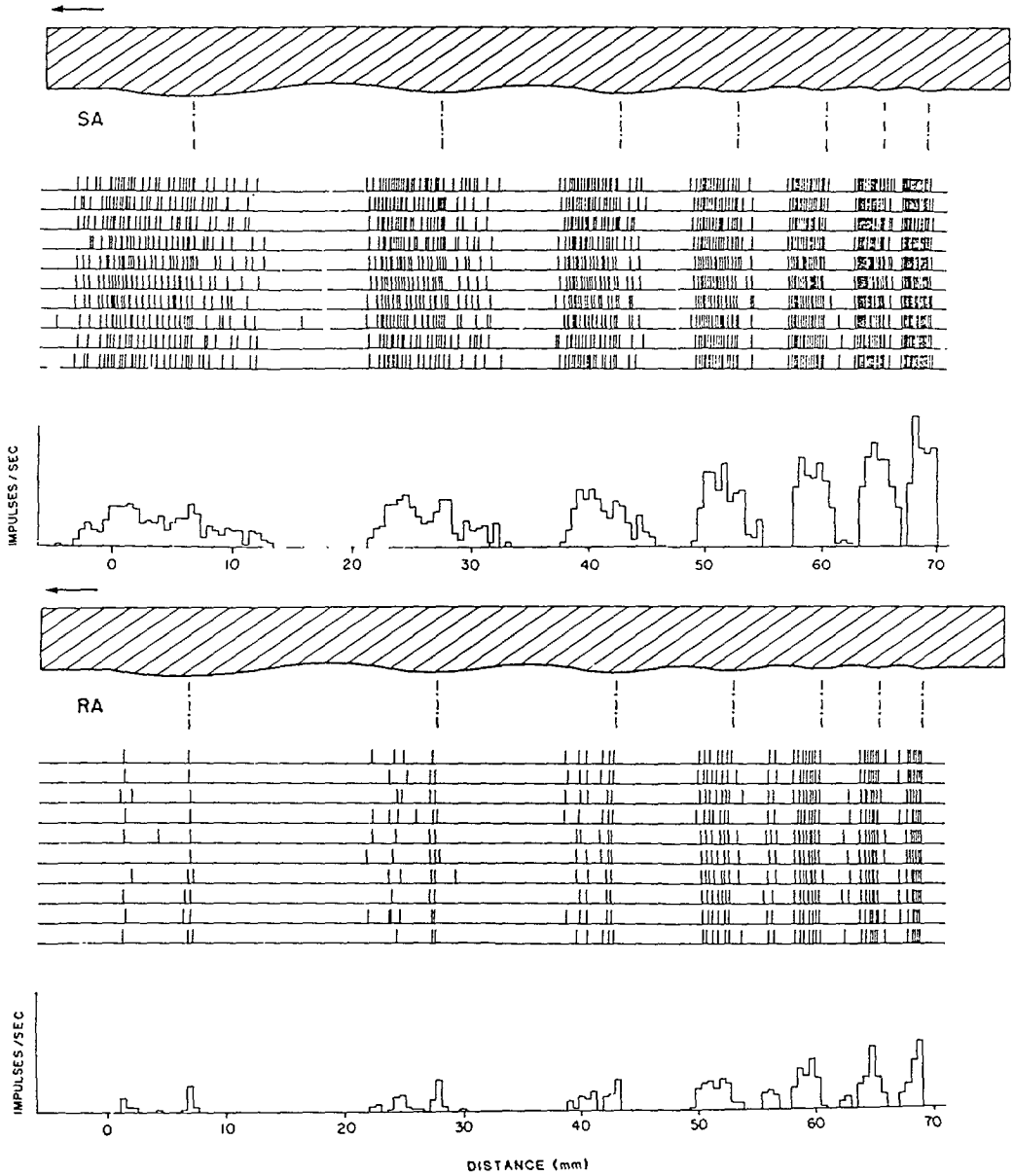

Fig. 4. SA and RA responses to a corrugated surface stroked under constant force. The vertical dashed lines immediately below the surface indicate the peaks of the ridges on the surface. The temporal sequence of action potentials, evoked by each of 10 strokes in the same direction, is plotted as a spatial sequence such that each tick mark represents the horizontal location of the MSS on the surface when an action potential occurred. A high degree of correlation is apparent between the frequency of action potentials and specific geometric features – the leading and trailing halves of the convex regions, and their curvatures. Histograms of the mean discharge rate per consecutive bins of 0.5mm are also shown.

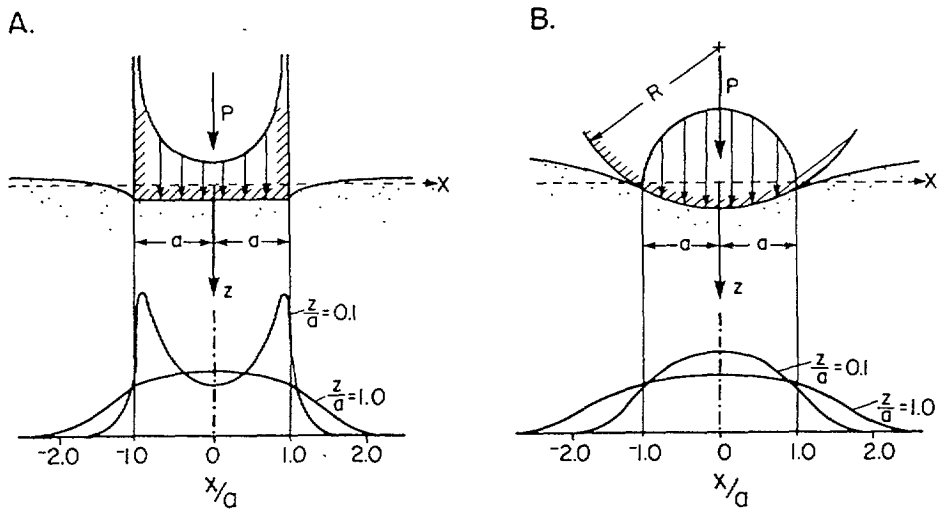

Fig. 5 The mechanics of contact between an elastic medium and rigid objects having rectangular (A) or circular (B) cross sections. The total force of indentation is P, and the width of the contact region is $2a$. X is the coordinate along the undeformed surface (shown by a dashed horizontal line), and Z is the depth of points below the surface. The deflected shape of the surface profile and the surface pressure distribution (indicated by the heights of equally spaced downward arrows superimposed on the object cross sections) are shown schematically. Also shown are the vertical or maximum strain (or stress) distributions at two arbitrary depths, illustrating the increase in blurring and loss of spatial detail as depth increases.

strains in the neighborhood of the receptors into trains of action potentials. The irregular three-dimensional geometry of the fingertip skin and subcutaneous tissues and the presence of large, time-dependent deformations whose spatial variations below the skin surface are unobservable, make both the experimental and theoretical biomechanical investigations complex. However, the salient features of the peripheral neural responses can be explained to surprising detail by the relatively simpler mechanistic analysis of idealized elastic media, as demonstrated first by Phillips and Johnson (1981b).

Two rigid indenters with shapes corresponding to the basic elements of the stimuli used by Phillips and Johnson (1981a), and in our neurophysiological experiments (sections 2 and 3) – a rectangular bar of arbitrary width and a circular cylinder of arbitrary radius – are shown indenting the surface of an elastic medium with a total force P in Fig. 5. Analyses based on the approaches devised by Hertz (1881) and Boussinesq (1885) show that the vertical pressure distribution on the skin under each of the indenters (assumed rigid and frictionless) is as shown (Gladwell, 1980). For the rectangular bar, the pressure at each corner is very high (theoretically infinite), while being minimum at the center. In contrast, for the cylindrical indenter, the pressure is zero at the two ends of the contact region, but is maximum at the center. Notice that whenever pressure peaks occur, either the curvature changes of the surface of the skin are higher (as under the corners of the rectangular bar), or the depth of indentation is higher (as under the

center of the cylinder) than the neighboring points. The pressure distributions on the skin surface give rise to normal and shear stress fields within the skin in the vertical and horizontal directions, which are related to the corresponding strain components through appropriate multiplicative constants related to the compliance of the elastic medium. Using the governing partial differential equations for the mechanical behavior of the medium, it can be shown that the medium acts as a low-pass filter for the mechanical signals (Srinivasan, 1989). Broadly speaking, this means that the distribution of the vertical or maximum normal stress, as well as strain (shown schematically in Fig. 5), on a horizontal plane inside the medium are blurred versions of the pressure distribution on the surface.

Consider the indentation of the skin by the rectangular bar of width $2a$ (Fig. 5A). The twin peaks in, for example, the maximum strain distribution, which are present very close to the surface (say, $Z/a = 0.1$), become blurred gradually as Z increases, and are absent when Z is high enough (say, $Z/a = 1.0$). For an alternative interpretation, let Z_0 denote the depth at which the Merkel cell (SA) receptors are located. Then, for wide enough bars Z_0/a is small, resulting in a strain profile that displays two peaks, where as for narrow bars Z_0/a is high, and the corresponding strain profile has only one peak. These results are consistent, with both the spatial response profiles of the SA, and the strain profiles obtained by Phillips and Johnson (1981a,b). For the indentation by a cylinder, it can be shown that for a given total force, the peak pressure varies inversely as the square root of the radius. Therefore, the higher the curvature of the cylinder, the higher the peak pressure, which, in turn, results in higher values of all the components of the stresses and strains at the receptor sites under the cylinder, thus explaining the higher discharge rate of the SA (Figs. 3 and 4). A similar explanation holds for the indentations by the sinusoidal steps described in section 1. For the RAs, which respond only to time-varying stimuli, the spatial distribution of the rate of change of pressure on the skin surface, and the resulting rates of change of stresses and strains at the receptor sites would be relevant.

5. Summary

Among the different possible geometric representations of the shape of objects, the intrinsic description, i.e., the surface curvature as a function of the distance along the surface, seems to be relevant for tactile sensing. Recordings of afferent responses to diverse shapes show that the depth of indentation and the change in curvature of the skin surface are represented in SA responses; in addition, the velocity and the rate of change in skin surface curvature are represented in both SA and RA responses. The primary reason for such neural encoding is the form of the spatial variation of the pressure imposed by the object on the skin surface: Pressure peaks occur where the depths of indentation and/or changes in the skin surface curvature are high. The skin effectively acts as a low-pass filter in transmitting the mechanical signals, and the mechanoreceptors respond to the blurred versions of the surface pressure distribution, thus encoding the shape of the object in terms of its surface curvatures.

References

Boussinesq, J. (1885). Application des Potentials a l'Etude de l'Equilibre et du Mouvement des Solides Elastiques, Gauthier-Villars, Paris.

Darian-Smith, I. and Kenins, P. (1980). Innervation density of mechanoreceptive fibers supplying glabrous skin of the monkey's index finger. J. Physiol. (Lond). 309, 147-155.

Gauss, C.F. (1827). Disquisitiones generales circa superficies curvas. Commentationes Societatis Regiae Scientiarum Gottingenesis Recentiores. 6, 99-146.

Gladwell, G.M.L. (1980). Contact problems in the classical theory of elasticity. Sijthoff and Noordhoff, Alphen aan den Rijn, The Netherlands.

Hertz, H.R. (1881). Ueber die Berührung fester elastischer Körper. J. reine u. angewandte Math. 92, 156-171. Also, Paper 5 of Volume 1 of collected works.

Horn, B.K.P. (1986). Robot Vision. M.I.T. Press, Cambridge, U.S.A.

Johansson, R.S. and Vallbo, A.B. (1979). Tactile sensibility in the human hand: Relative and absolute densities of four types of mechanoreceptive units in glabrous skin. J. Physiol. (Lond). 286, 283-300.

Knibestöl, M. (1973). Stimulus-response functions of rapidly adapting mechanoreceptors in the human glabrous skin area. J. Physiol. (Lond). 232, 427-452.

Knibestöl, M. (1975). Stimulus-response functions of slowly adapting mechanoreceptors in the human glabrous skin area. J. Physiol. (Lond). 245, 63-80.

LaMotte, R.H. and Srinivasan, M.A. (1987a). Tactile discrimination of shape: Responses of slowly adapting mechanoreceptive afferents to a step stroked across the monkey fingerpad. J. Neuroscience. 7, 1655-1671.

LaMotte, R.H. and Srinivasan, M.A. (1987b). Tactile discrimination of shape: Responses of rapidly adapting mechanoreceptive afferents to a step stroked across the monkey fingerpad. J. Neuroscience. 7, 1672-1681.

LaMotte, R.H. and Srinivasan, M.A. (1990). Surface microgeometry: tactile perception and neural encoding. This volume.

Phillips, J.R. and Johnson, K.O. (1981a). Tactile spatial resolution II. Neural representation of bars, edges, and gratings in monkey primary afferents. J. Neurophysiol. 46, 1192-1203.

Phillips, J.R. and Johnson, K.O. (1981b). Tactile spatial resolution III. A continuum mechanics model of skin predicting mechanoreceptor responses to bars, edges, and gratings. J. Neurophysiol. 46, 1204-1225.

Pubols, B.H. Jr. and Pubols. L.M. (1976). Coding of mechanical stimulus velocity and indentation depth by squirrel monkey and raccoon glabrous skin mechanoreceptors. J. Neurophysiol. 39, 773-787.

Srinivasan, M.A. (1989). Tactile sensing in humans and robots: Computational theory and algorithms. Newman Lab. Tech. Report, Dept. of Mech. Eng., M.I.T., Cambridge, U.S.A.

Srinivasan, M.A. and LaMotte, R.H. (1987). Tactile discrimination of shape: Responses of slowly and rapidly adapting mechanoreceptive afferents to a step indented into the monkey fingerpad. J. Neuroscience. 7, 1682-1697.